

THE TILT ANGLE TRANSITION AND POTENTIAL FLOW

by Daniel D. Joseph

Department of Aerospace Engineering and Mechanics
University of Minnesota, Minneapolis, MN 55455 USA

Lecture presented at the NSF-DOE Workshop on
Flow of Particulates and Fluids
NIST, Gaithersburg, MD
September 17, 1992

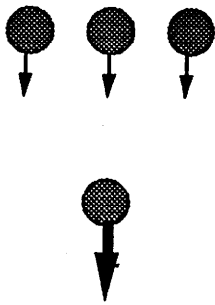
The natural orientation of a long body is the key to understanding flow induced structures of spherical bodies. The natural orientation of a long body falling in a viscous liquid is broadside-on; the body will always turn its longside perpendicular to the stream. The same body falling slowly in a viscoelastic liquid will turn its longside parallel to the stream, perpendicular to the orientation in a viscous liquid. Spheres falling in a viscous liquid have a tendency to align across the stream like a long body. The mechanism which leads to cross stream arrays is drafting, kissing and tumbling.

One sphere is attracted into the wake of another; they are sucked together in the drafting part; then they kiss and momentarily form a long body aligned with the stream which is unstable and turns broadside-on (Fortes, Joseph and Lundgren [1987]; Joseph, Singh and Fortes [1992]). The drag on the cross stream array is larger than on a single sphere so that a single sphere falls faster (Figure 1). It is altogether different in a viscoelastic liquid in which spheres align with rather than across the stream. Chains are long bodies aligned with the stream which are stable when they fall slowly in a viscoelastic fluid. The drag on a chain of spheres is much less than the drag on one (Figure 1).

Long bodies which fall faster in a viscoelastic liquid will undergo a tilt transition (Joseph, Nelson, Hu and Liu [1992]). Tilt angles of long cylinders falling in aqueous solutions of polyox and polyacrilamide were measured by Liu and Joseph [1992]. The effects of particle length, particle weight, particle shape, liquid properties and liquid temperature were determined. In these experiments, the cylinders fall under gravity in a two-dimensional bed. No matter how or where they are released they will center themselves between the close walls and fall steadily in a configuration in which the axis of the cylinder is at a fixed angle of tilt with the horizontal. A discussion of the tilt angle may be framed in terms of competition between viscous effects, viscoelastic effects and

DRAG

NEWTONIAN



A single particle falls *faster* than the cross stream array. The drag on many is *greater* than the drag on one.

VISCOELASTIC



A single particle falls *slower* than a chain of spheres. The drag on many is *less* than the drag on one.

Figure 1. Drag on many spheres and a single sphere in Newtonian and Viscoelastic liquids.

inertia. When inertia is large the particles settle with their broadside perpendicular to the direction of fall. When inertia is small viscoelasticity dominates and the particles settle with their broadside parallel to the direction of fall. The tilt angle varies continuously from 90° when viscoelasticity dominates to 0° when inertia dominates. The balance between inertia and viscoelasticity was controlled in the experiments of Liu and Joseph [1992] by systematic variation of the weight of the particles, the concentration of polyox in water and of the temperature of the solution. Particles will turn broadside-on when the inertia forces are larger than viscous and viscoelastic forces. This orientation occurred when the Reynolds number was greater than some number not much greater than one in any case, and less than 0.1 in Newtonian liquids and very dilute solutions. The appearance of a tilt angle, however, appears to be most strongly correlated with values of a viscoelastic Mach number $M=U/c$ where U is the terminal velocity and c is the shear wave speed measured with the shear wave speed meter (Joseph [1990]). Strong departure of the tilt angle from $\theta = 90^\circ$ begins at about $M=1$ and ends with $\theta = 0^\circ$ when $1 < M < 4$. The dynamics which controls this orientation transition is provisionally interpreted as a change of type. When M is increased past one the vorticity equation for steady flow becomes hyperbolic in certain regions of the flow. The flow in front of the body then becomes irrotational. The inertial couples at the irrotational forward side of the body which turn a body broadside-on in a viscous fluid can then also operate in the supercritical viscoelastic case.

The scenario we have described in the preceding paragraph leads us to a discussion of potential flow of a viscoelastic fluid. It is possible to work a complete theory of potential flow for a second order fluid (Liao and Joseph [1992]) and a linear viscoelastic fluid (section 5). There is an additional term in the Bernoulli equation for a second order fluid, but the viscosity does not enter. The drag on a body in the potential flow of a second order fluid is the same as an inviscid potential flow. The lift on two-dimensional bodies is given by the usual Kutta condition but the moment about the origin of the stresses acting on the body is given by $M_I + 2 \mu \Gamma + 2 \alpha_1 \frac{\partial \Gamma}{\partial \tau}$ where M_I is the usual moment for an inviscid fluid, Γ is the circulation, μ is the viscosity and $-\alpha_1 = n_1 / 2$ where n_1 is the zero shear coefficient of the first normal stress. There is therefore an additional moment $2 \mu \Gamma$ due to viscosity when $\alpha_1 = 0$ as in a Newtonian fluid.

1. Introduction

Michele, Pätzold and Donis [1977] have noted that small spheres ($\sim 70 \mu\text{m}$) in an oscillating liquid sheared by the back and forth motion of parallel plates, or cone and

plates (Highgate [1966], Highgate and Whorlow [1969], Petit and Noetinger [1988]) align in the direction of shear when the liquid is viscoelastic and across the direction of shear when the liquid is Newtonian (Petit and Noetinger [1988]). In a different kind of experiment involving steady flow without shear, Joseph, Nelson, Hu and Liu [1992] showed that large spheres several millimeters in diameter sedimenting in a fluid-filled channel will arrange themselves so that the line of centers between neighboring spheres is across the stream in a viscous liquid and parallel to the stream in a viscoelastic liquid when the fall velocity is small but across the stream again when the fall velocity is large. They noted that this flow-induced anisotropy of sedimenting spheres is associated with the natural orientation of long bodies with their broadside parallel to the stream when viscoelasticity dominates and perpendicular to the stream when inertia dominates. Chains of spheres can also be seen in the sketches of the paper by Allen and Uhlherr [1989], but they were not identified in the text of that paper. In the present paper we focus on the orientation effects of sedimenting long bodies.

It is well known that the orientation of sedimenting long bodies in Stokes flow is undetermined; there are no hydrodynamic couples to turn a long body in steady flow. It is also known that flows of many different viscoelastic fluids reduce to Stokes flow when the flows are sufficiently slow and slowly varying. Turning couples appear at 2nd order.

Leal [1975] has studied the sedimentation of slender bodies in a second order fluid with inertia neglected. He considers only those non-Newtonian effects resulting from the disturbance velocity field generated by the lowest order geometry-independent approximation of the Stokeslet distribution used in slender body theory. He finds that freely translating particles with fore-aft symmetry exhibit a single stable orientation with the axis of revolution vertical. This suggests that the angle θ of tilt observed in experiments may be determined by a competition between inertia and viscoelasticity. The mechanism which aligns a slender body with the stream is not easy to extract from Leal's analysis. Brunn [1977] worked an asymptotic theory in powers of the Weissenberg number with inertia neglected and found that to leading order a transversely isotropic particle will change its orientation until it becomes either parallel or perpendicular to the direction of the external force. An excellent review of what is known about the slow motions of particles in non-Newtonian fluids with inertia neglected was given by Leal [1979].

Inertia cannot be neglected in a general discussion of the orientation of sedimenting long bodies. The streamwise orientation of a long body is unstable in a viscous liquid; the body will always turn its broadside to the stream. An explanation (Thompson and Tait [1879]) for this can be found in the couples which are produced by high pressures at the stagnation points on the long body shown in Figure 2. Potential flow

is probably a good approximation for viscous flow on the forward side of the body. If the pressures outside a thin boundary layer at the stagnation points were reversed, the long body would not put its broadside into the stream, but instead would put its broadside parallel to the stream, as is in fact the case in the settling of long cylinders in various viscoelastic liquids.

The potential flow mechanism for turning long bodies broadside on cannot provide the whole explanation at finite Reynolds numbers. In practice, wakes and skin friction enter into the description. Viscous tractions are not negligible, even at the front of the ellipse. Stokes flows around transversally isotropic bodies like cylinders and ellipsoids of revolution which have fore and aft symmetry are symmetric in the sense that the sum of moments of traction vectors on the boundary of the body vanish. Inertia destroys this symmetry and generates a net turning couple which turns the broadside of the body into the stream. Inertia leads to strong moments when viscosity is neglected and viscosity leads to zero net moment when inertia is neglected.

The hydrodynamics of the couples which turn sedimenting and fluidized long bodies at a finite Reynolds number are not understood in detail. However, a detailed description can be obtained in two dimensions from the direct numerical simulation of the motion of a sedimenting ellipse given by Hu, Joseph and Crochet [1992]. They developed a package that simulates the unsteady two-dimensional solid-liquid two-phase flow using the Navier-Stokes equations for the liquid and Newtons equations for the solid particles. Hu, Joseph and Fortes [1992] presented a paper and video tape of this simulation for the case in which a 2/1 ellipse whose density $\rho = 1.2$ is greater than water, is dropped from rest with its longside parallel to gravity in a channel whose width is 4 times greater than the long side of the ellipse. You may see how the ellipse turns its broadside into the stream as it rocks due to vortex shedding at a Reynolds number $Re = 60$ (based on the terminal velocity and the length of the major axis) in the video and as shown in Figures 3 and 4 where we have plotted the dynamic pressure distribution and isobars at different times. We are going to do more, including plots of streamlines and the distribution of moments due to pressures, normal and shear tractions, in a future publication. Figures 3a,b are for early times and 4a,b for later times after transients have decayed. The pictures are indexed for equal times by an integer valued index, i_{time} . Even at the earliest time $i_{time} = 1$, the dynamic pressure does not exhibit the recovery expected for potential flow. To see how turning couples due to pressure work at early time, it is best to take moments about the center. We can see that the relatively high pressures near to the point at the front on the right ($125^\circ < \theta < 180^\circ$) which would be the forward stagnation point in potential flow contributes strongly to the turning couple.

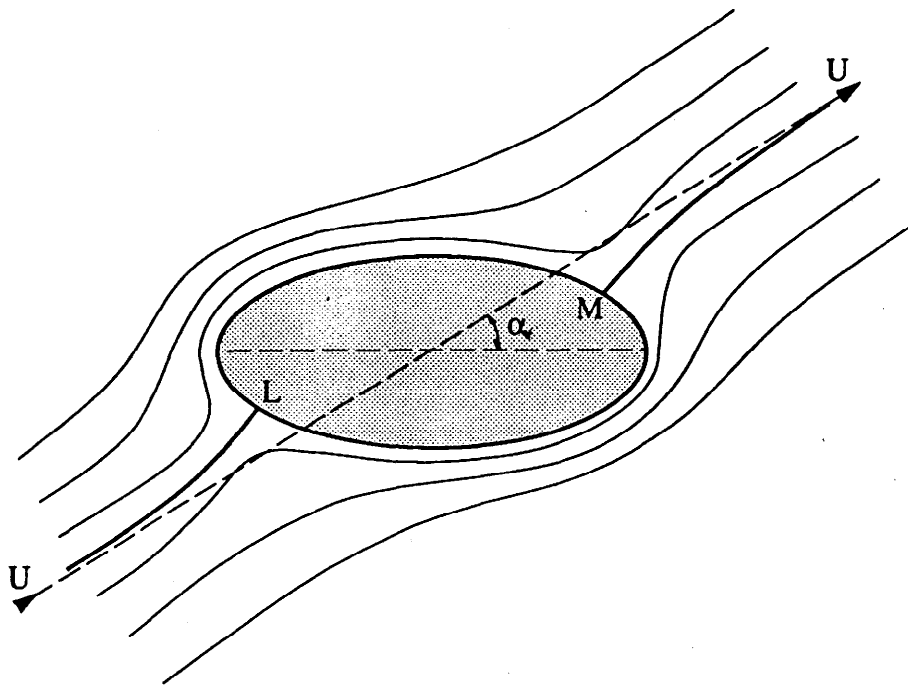


Figure 2. Potential flow past a cylinder. The pressure at stagnation points L and M will turn the broadside of the body into stream. If the extensional stress at L and M were reversed, as may be possible in a viscoelastic liquid, the body would line up with the stream.

The orientation of a long body settling in a liquid under gravity is equivalent to the steady flow past a stationary long body. This latter problem has been treated in works of Ultman and Denn [1970], Joseph [1985], Crochet and Delvaux [1990], Hu and Joseph [1990] and Fraenkel [1988,1991]. These studies and related matters are discussed in the book of Joseph [1990]. The nonlinear studies were based on the upper-convected Maxwell model, but the linearized studies were basically model-independent. They show that the flow goes supercritical when the viscoelastic Mach number $M=U/c$ passes through one; the vorticity equation of the steady flow changes type from elliptic when $M<1$ to hyperbolic when $M>1$. The condition $M>1$ also arises from the condition that an elastic length λU is greater than a viscous length ν/U where λ is a relaxation time, ν is the kinematic viscosity and $C^2 = \nu/\lambda$. In the supercritical case there is a Mach cone of vorticity.

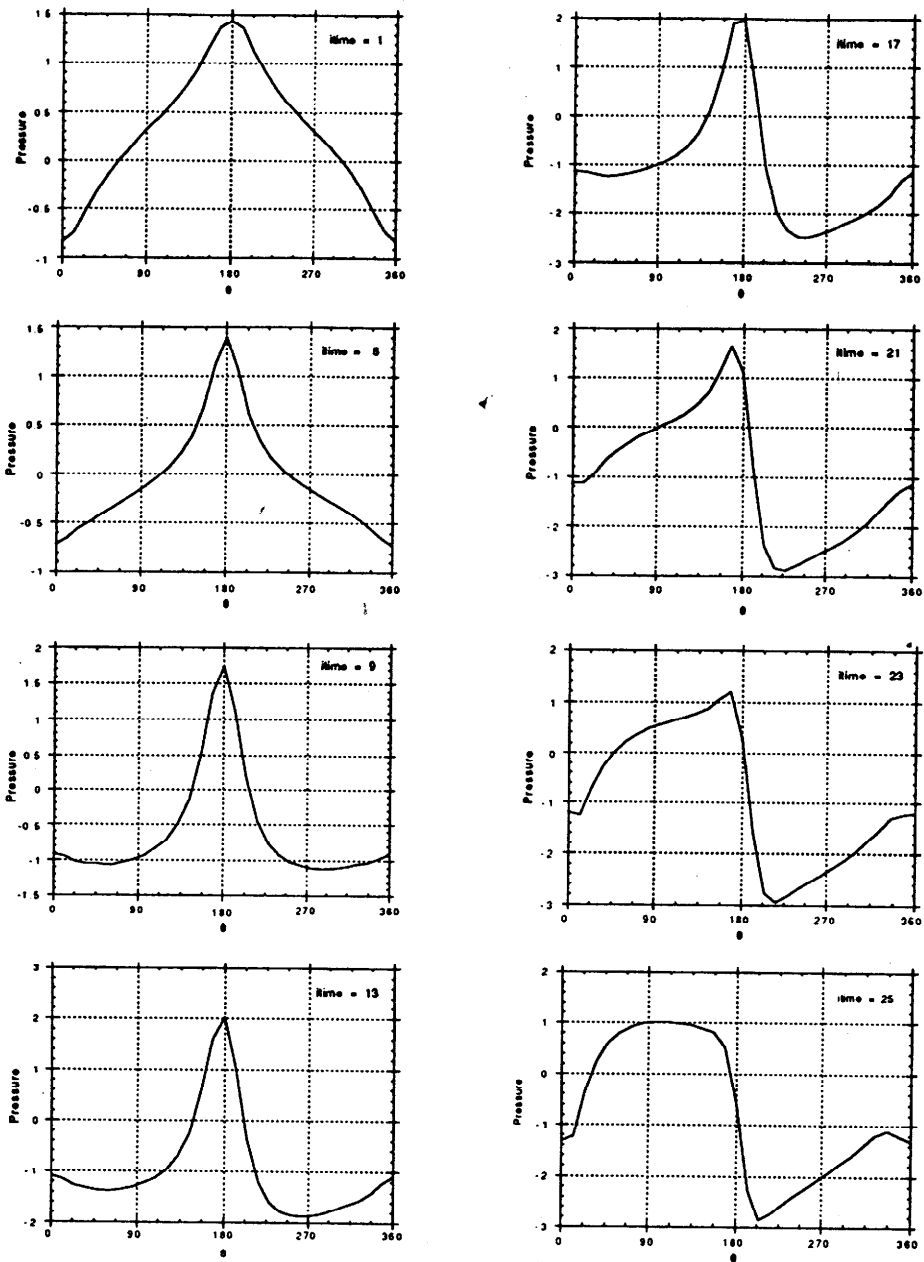


Figure 3a. Pressure distribution on the surface of a 2:1 ellipse for the early stage of its settling. $\theta = 0$ is the upper end point of the long axis at the beginning and θ increases clockwise.

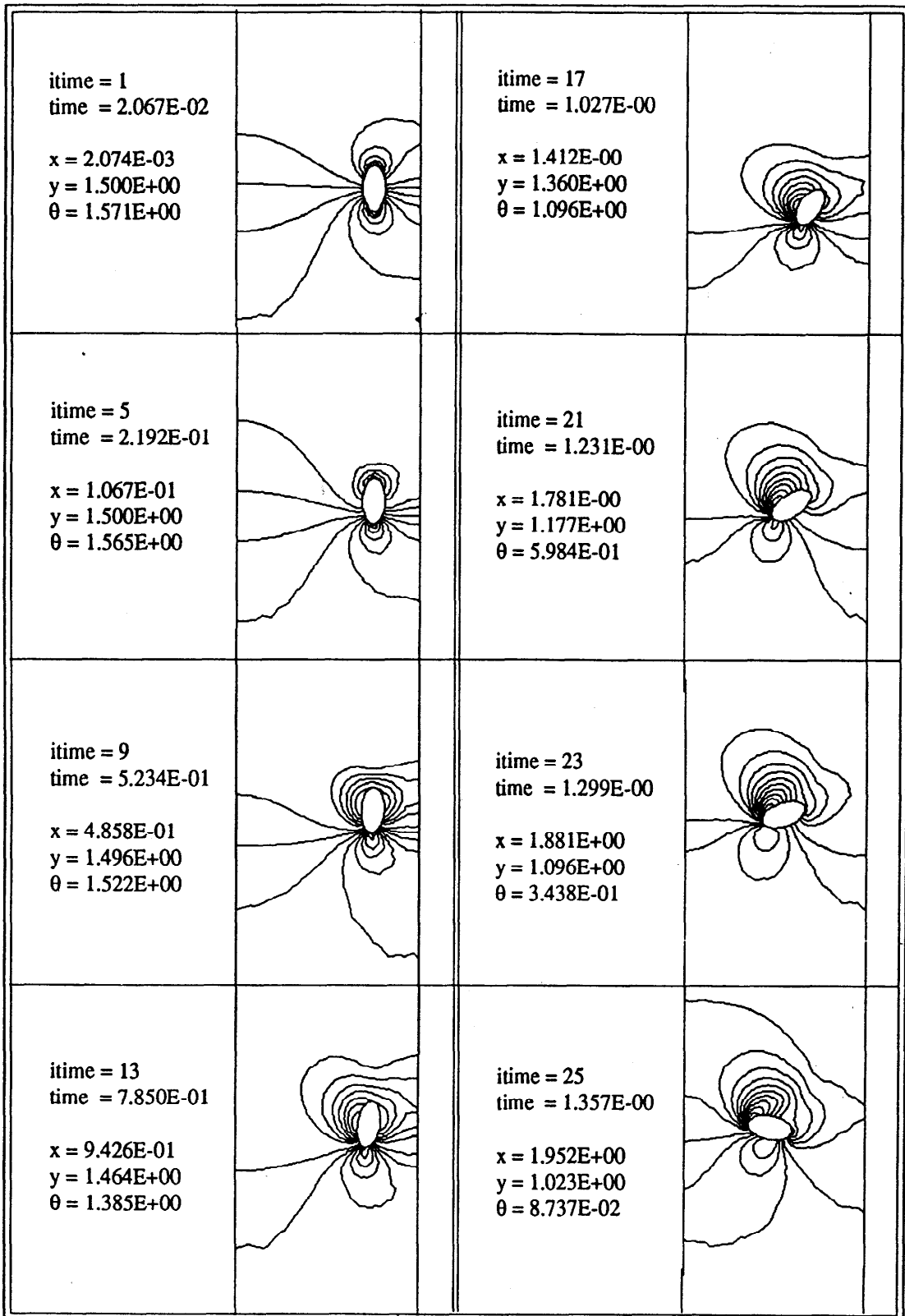


Figure 3b. Pressure Contours at the Early Stage of the Settling of a 2:1 Ellipse. Terminal $Re = 60$. (x,y) indicates the position of the center of the ellipse and θ the angle.

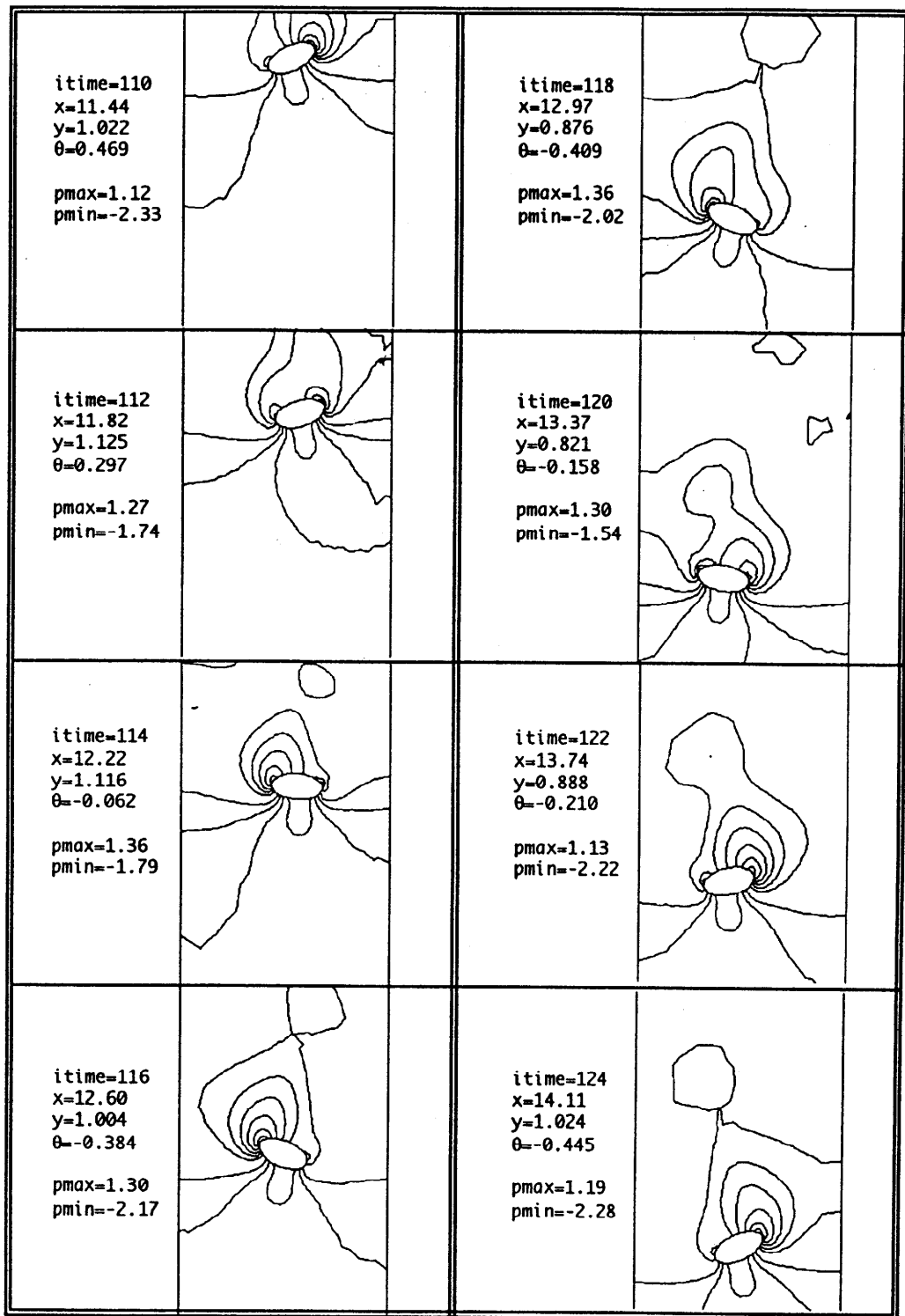


Figure 4a. (Hu, Joseph and Fortes, 1992) Pressure contour plots for a sedimenting ellipse during a cycle of rocking at $Re=60$. (x,y,θ) indicates the position of the ellipse. p_{max} and p_{min} are the maximum and minimum values of the dynamic pressure at each instant. From p_{min} to p_{max} there are nine equally spaced isopressure lines in each plot with high pressure in front.

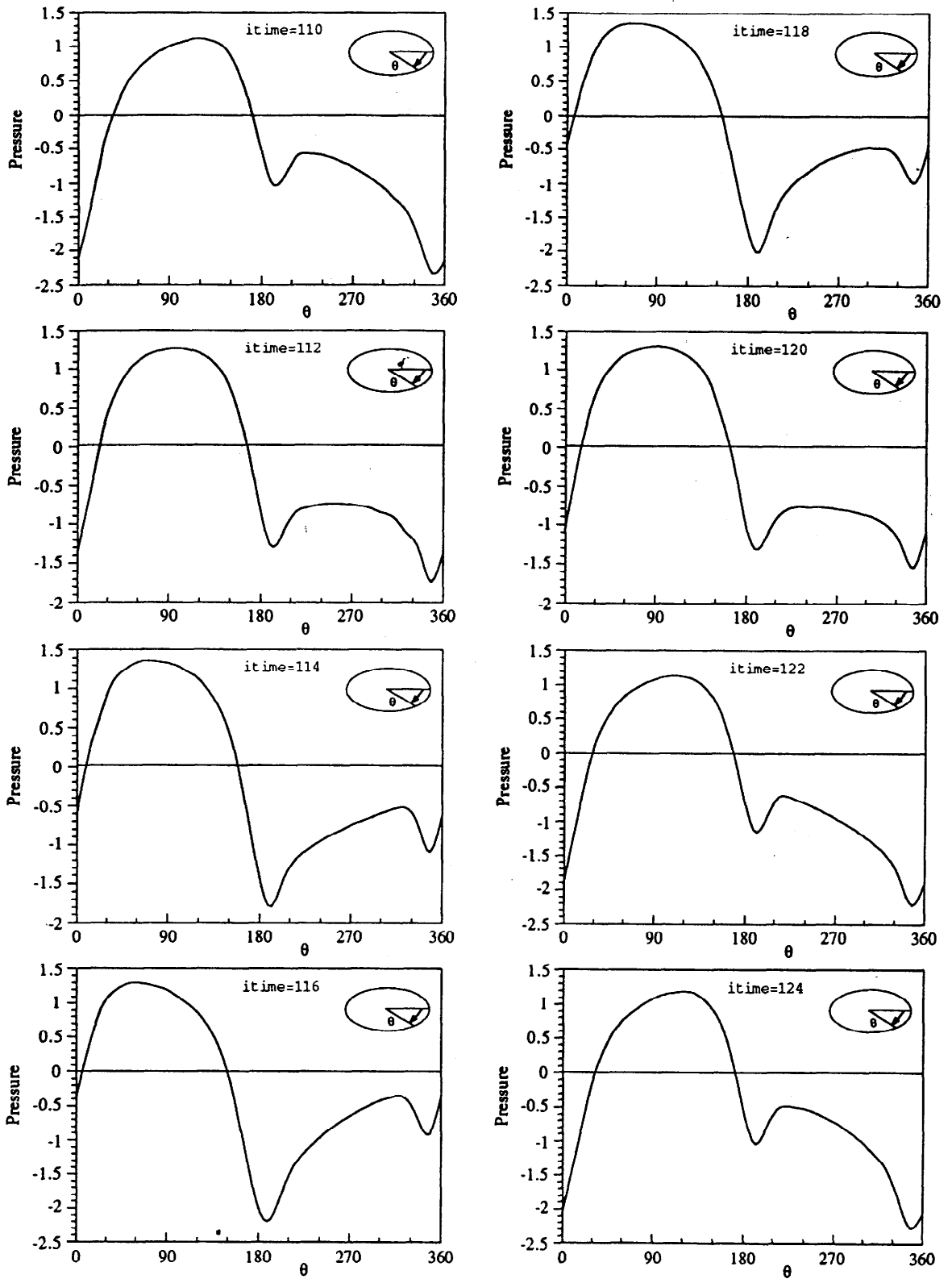


Figure 4b. (Hu, Joseph and Fortes, 1992) Pressure distribution on the surface of the ellipse for the times shown in figure 2. The two peaks of negative pressure on the back of the ellipse control the turning of the ellipse.

In front of the cone there is a "region of silence," actually potential flow, with vortical flow behind the cone. The supercritical transitions do seem to correspond to the flow transitions observed in the experiments on the flow over wires reported by James [1967], James and Acosta [1970] and Ambari, Deslouis and Tribollet [1984], as well as to the flow features observed in the experiments on flow over flat plates of Hermes and Fredrickson [1967].

The change of orientation of long bodies sedimenting in aqueous solutions of polyox can be framed as a change of type with features resembling those already seen in studies delayed die swell (see, Joseph [1990], henceforth called I). The cylinders settle vertically, more or less, when the Mach number is less than some number not too much greater than one. When Mach number is larger than about three the particles have all turned their broadside to the stream, evidently controlled by inertia. Potential flow enters naturally into this description because there is an irrotational flow with a large upstream influence in front of the shock.

2. The tilt transition

The tilt transition has already been described in the summary at the beginning of this paper. Cylinders sedimenting slowly in a viscoelastic liquid will turn to put their longside parallel to gravity (Leal 1975, Brunn 1977). Heavier cylinders which fall faster put their longside perpendicular to gravity. Cylinders which fall faster than those which fall straight down but slower than those which fall broadside on fall with fixed angle of tilt as shown in Figure 5. The angle of tilt varies continuously with speed from straight down to broadside on. The transition occurs in a narrow range of speeds and can therefore be studied for critical conditions. Liu and Joseph [1992] showed that the tilt transition could be traversed in a single fluid by varying the weight of the particle, or with one single fluid by varying the temperature of the solution, or with one single particle at a single temperature by varying the concentration of the solution.

Many of the essential features of the tilt transition can be determined by careful study of Figure 6 in which the angle of the tilt is plotted against a Reynolds number $\mathbb{R} = U\ell/(\eta/\rho)$ where U is the terminal speed of the particle, η/ρ is the kinematic viscosity and ℓ is the hydraulic diameter. In aqueous polyox with concentrations ranging from 0.6 to 1.5%, the cylinders fall straight down when \mathbb{R} is smaller than a value near one and turns broadside for large Reynolds number exceeding 10. The Reynolds number can be interpreted as the ratio of the fall speed to a diffusion speed $\eta/\rho\ell$. So the tilt transition occurs when the fall velocity exceeds the diffusion velocity in the viscous case. This interpretation is definitely conditional because the cylinder will always turn its broadside to the stream eventually no matter how small $\mathbb{R} > 0$ may be. Inertia will ultimately have

its way. We have to consider the nature of the forces which hold the long particle vertical in a viscoelastic fluid when the Reynolds number is finite and not too large.

The results suggested by Figure 6 are general and definitely not restricted to one or even a family of viscoelastic liquids.

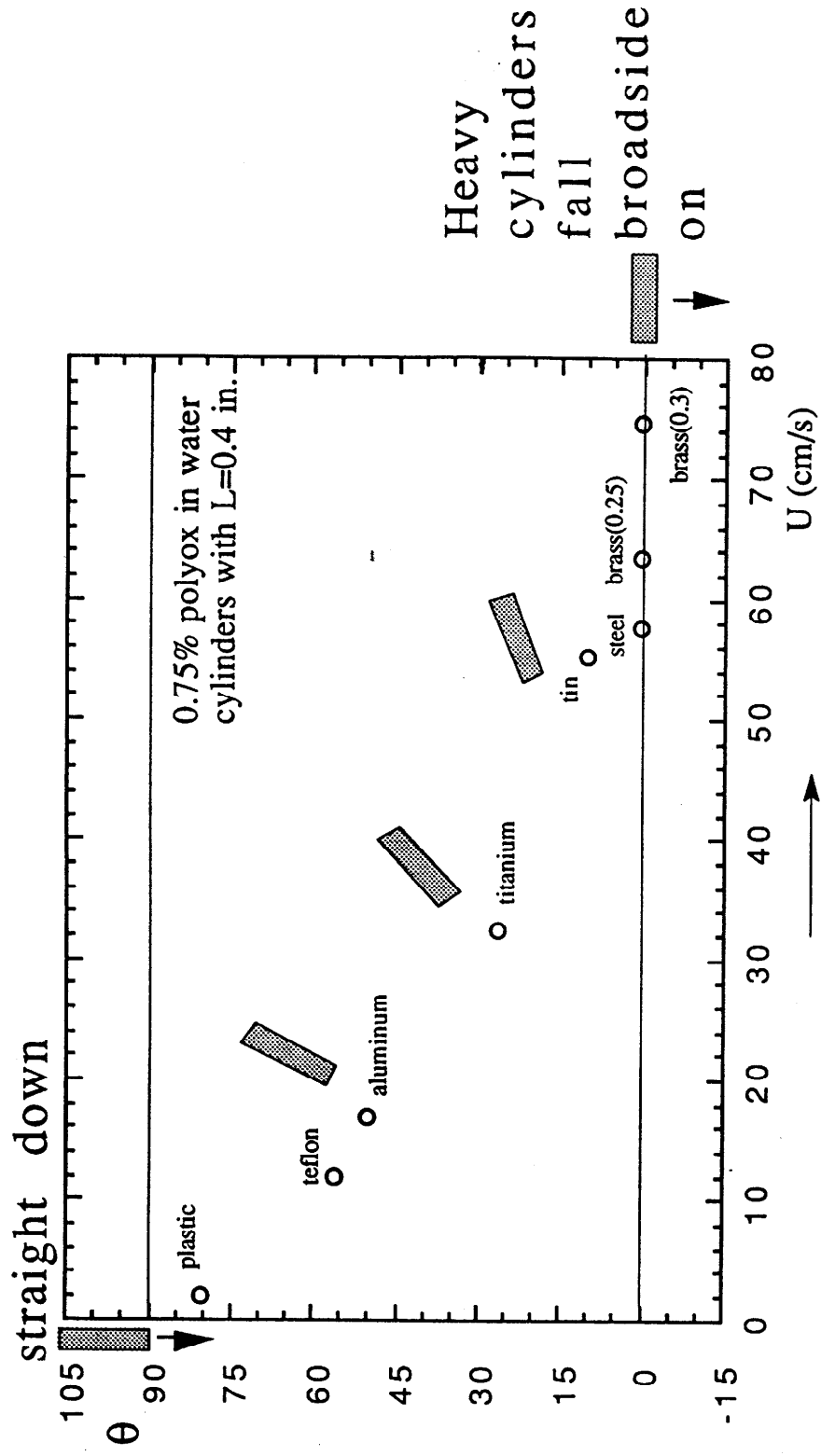
3. The tilt transition and change of type

Liu and Joseph [1992] interpreted the tilt transition as a change of type analogous to transitions between subsonic and supersonic flow in gas dynamics. An examination of some mathematical issues involved in problems of change of type will be given in section 4 and a more detailed explanation can be found in the book by Joseph [1990]. For now it will suffice to organize the data on the tilt transition in terms of the viscoelastic Mach number $M = U/c$ where c is the "shear wave" speed measured on the wave speed meter (see Joseph, Riccuis and Arney [1986], Joseph [1990]). In the tilt experiments c carries between 10 and 20 cm/sec.

The speed of a shear wave into a fluid at rest is given by $c = \sqrt{G/\rho}$ where G is the shear modulus of the fluid which for Maxwell models is given by $c = \eta/\lambda$ where η is the viscosity and λ the relaxation time. The measurement of c could hardly be more important. Aerodynamics would look good on paper, but only there, if we could not measure the speed of sound. Of course, the speed of sound is "infinite" in incompressible fluid so that only shear waves (more correctly, vorticity waves) can propagate. The wave speed meter measures transit times. Nothing happens for a time after an impulsive bang, but finally the detector picks up a signal and we can measure a time of transit which we call a wave when the distance traveled over the transit time is the same for different distances. Bangs are what you get in nature and the speeds we measure seem to be more correlated with dynamics than the phase speeds one measures on more delicate instruments in which the frequencies are controlled. The relaxation time $\lambda = \eta/\rho c^2$ which we compute from measured values of c are at least an order of magnitude smaller than the times measured by the usual methods. In fact the usual rheometers don't even begin to work at times much less than 10^{-2} seconds in which most of the stress relaxation has already occurred.

Figure 7 presents the same data as in Figure 6, but it is plotted against the Mach number. There is a very sharp transition from parallel to perpendicular falls for M slightly larger than one. An even sharper transition of the same type is exhibited in the 1.2% aqueous polyacrilamide shown in Figure 8. Similar results are displayed by Liu and Joseph [1992] for polyox in glycerin solutions.

Light cylinders fall straight down



Heavy cylinders fall faster

Figure 5. (Liu and Joseph, 1992) The tilt transition. Cylinders fall with a fixed angle of tilt in 0.75% aqueous polyox.

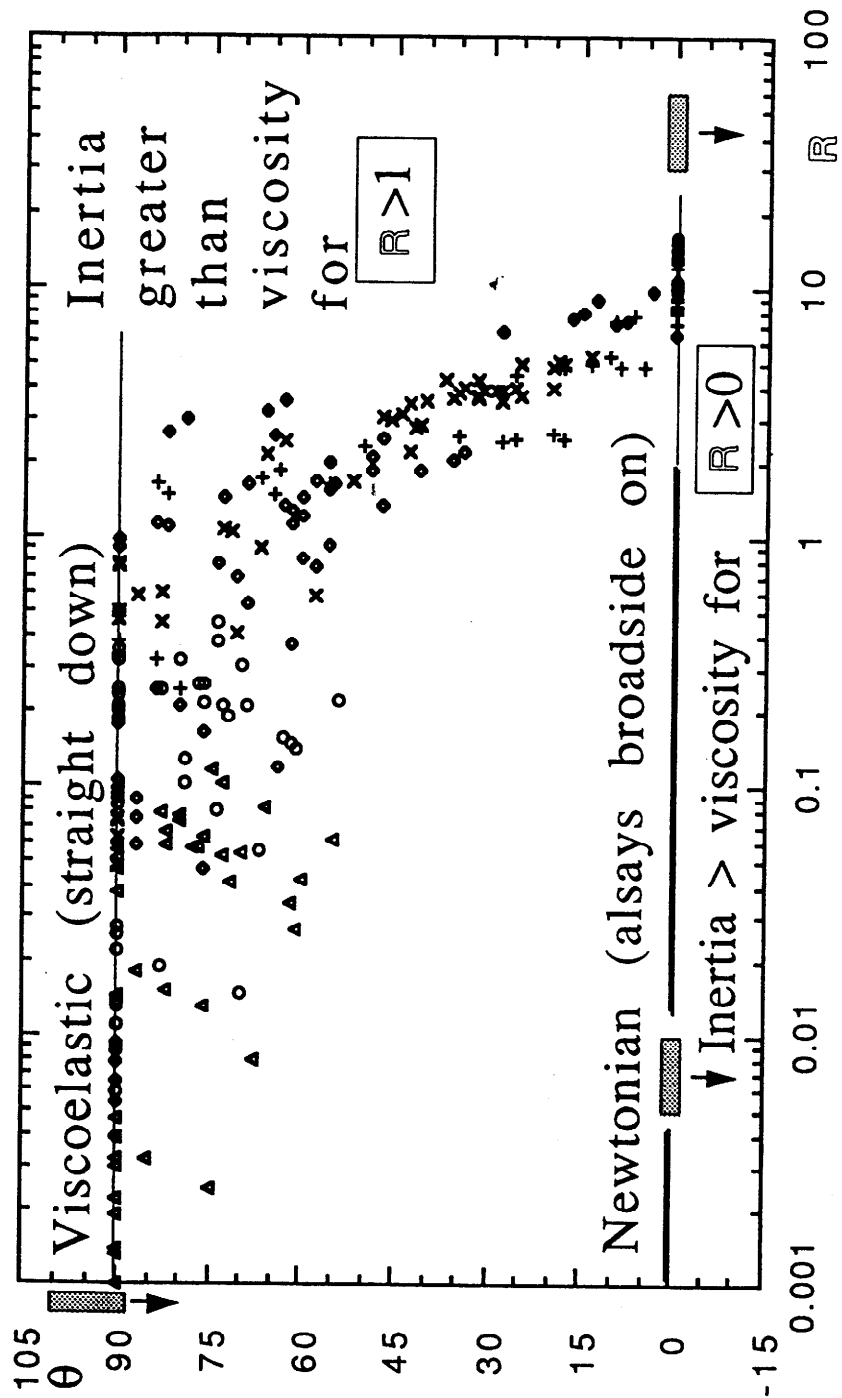


Figure 6. Tilt angle θ vs. Reynolds number for all data, cylinders of all length, shapes and weights in polyox/water solutions. Δ 1.5%, \diamond 0.85%, \times 1%, $+$ 0.75%, \bullet 0.5%.

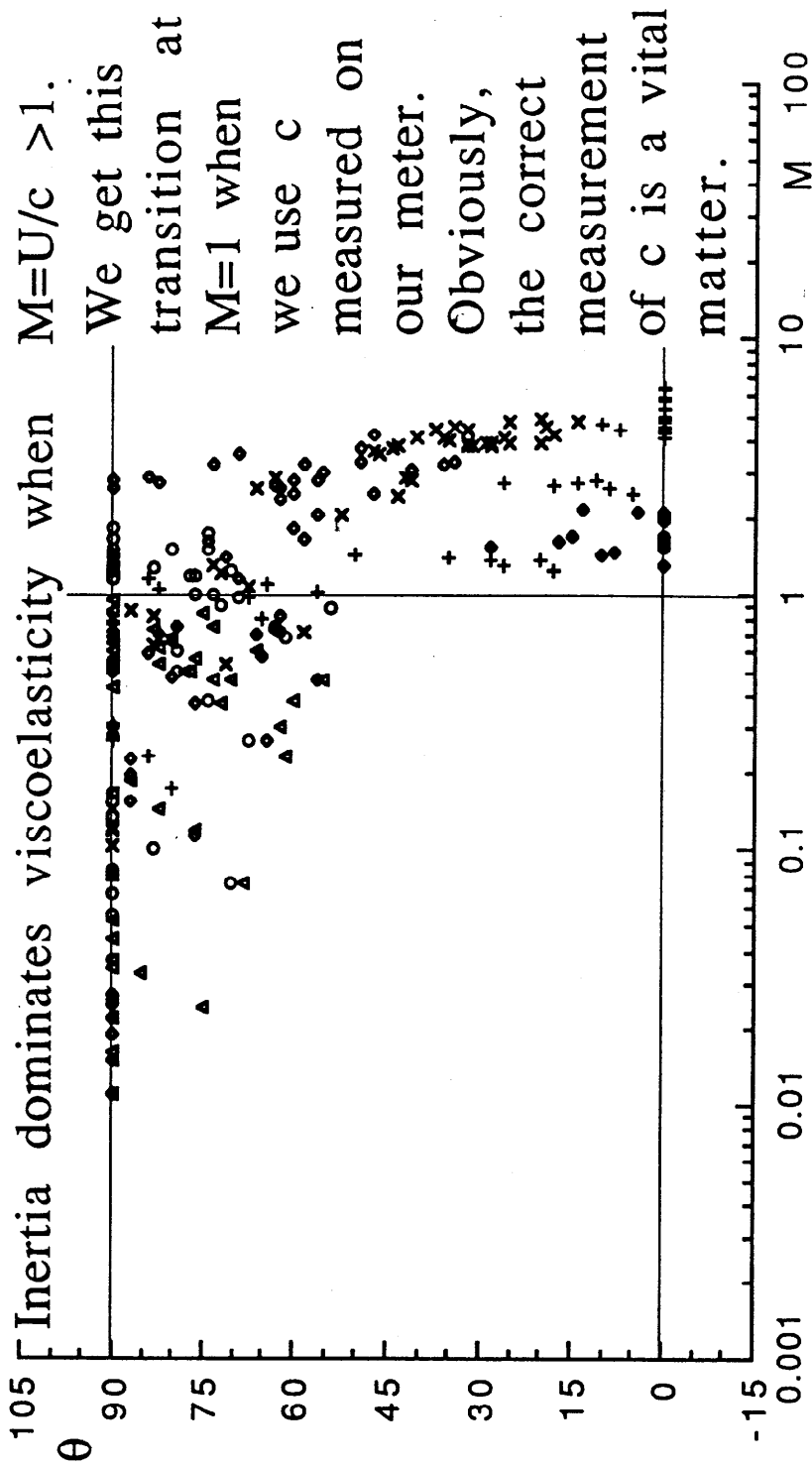


Figure 7. Tilt angle θ vs. Mach number for all the data, cylinders of all length, shapes and weights in polyox/water solutions. Δ 1.5%, \circ 1.25%, \diamond 0.85%, \times 0.75%, $+$ 0.6%, \bullet 0.5%.

viscoelasticity > inertia
 $M < 1$

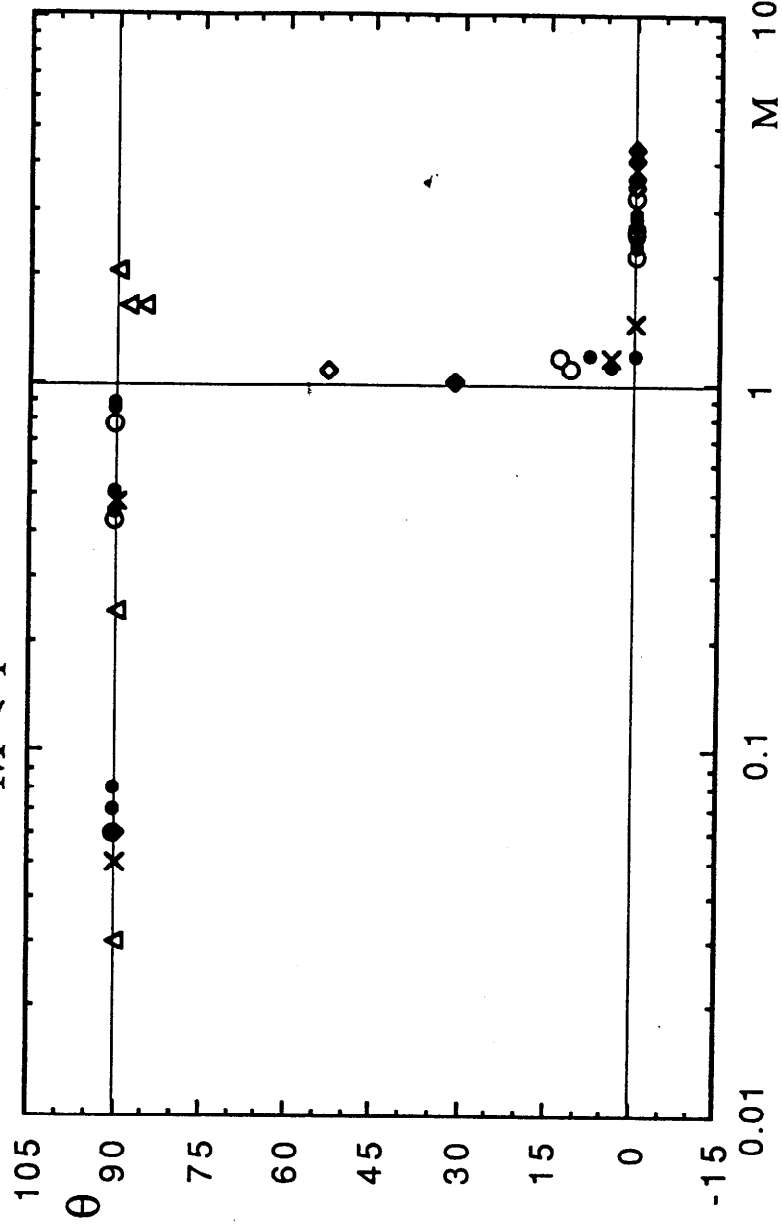


Figure 8. Tilt angle θ vs. Mach number for cylinders with $L=0.8$ in. (most with round ends) in 2% aqueous polyacrylamide
 Δ $D=0.1"$, \times $0.15"$, \bullet $0.25"$, \circ $0.25"$ (flat ends), \diamond $0.35"$, \blacklozenge $0.4"$.

We may interpret the data to say a tilt transition does not occur until $M = 1$ at least. $U > c$ may be interpreted as expressing the dominance of inertia over viscoelasticity. Here the diameter of the cylinder and other features enter the criteria through the terminal velocity alone, since the shear wave speed is a material parameter. It is a rather demanding criterion since it requires that the transition should occur only when the fall velocity exceeds a speed determined by the material and not by the experiment.

In Newtonian fluids there are no shear waves; changes in shear are propagated as diffusion. It is necessary to define a conceptual framework to bridge the gap between Newtonian and viscoelastic fluids. The traditional way to bridge this gap is with models like Jeffreys which combine elasticity and diffusion (see Joseph [1990] for a full discussion). A popular constitutive equation of the rate type in which elasticity and diffusion can both act is the Oldroyd B. This can be written as

$$\lambda \overset{\Delta}{\tau} + \tau = \eta \mathbf{A}[\mathbf{u}] + \lambda_2 \overset{\Delta}{\mathbf{A}}[\mathbf{u}] \quad (3.1)$$

where $\mathbf{A}[\mathbf{u}] = \mathbf{L}[\mathbf{u}] + \overset{T}{\mathbf{L}}[\mathbf{u}]$ and $\mathbf{L} = \nabla \mathbf{u}$, where \mathbf{u} is the velocity. Here Δ stands for an upper convected derivative,

$$\overset{\Delta}{\sigma} \stackrel{\text{def}}{=} \frac{\partial \sigma}{\partial \tau} + (\mathbf{u} \cdot \nabla) \sigma - \mathbf{L} \sigma - \sigma \overset{T}{\mathbf{L}}, \quad (3.2)$$

λ is a relaxation time and λ_2 is a retardation time. Equation (3.2) reduces to a Maxwell model when $\lambda_2 = 0$ and to a Newtonian fluid when $\lambda_2 = \lambda$. Small values of $\lambda_2 = \lambda$ can be regarded as viscous perturbations of viscoelasticity.

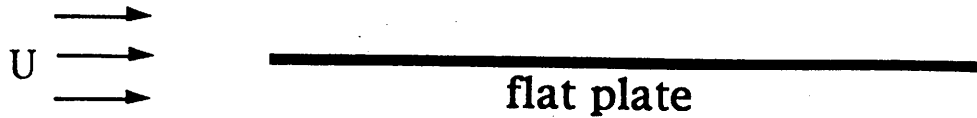
It is not unlikely that careful study of the tilt transition in semi-dilute solutions can reveal important properties of fluids in which the action of elasticity and diffusion are both important.

4. Partly hyperbolic linearized flow over a flat plate

If you drop a light, thin, flat plate in a viscoelastic liquid it will fall with its broadside parallel to the stream and its longside down. A heavy plate will turn broadside on and the transition between the two modes of falling appears to be a change of type, mean $M = 1$. The problem of flow over a flat plate has been studied by Hermes and Fredrickson [1967], Joseph [1985 and 1990] and Fraenkel [1988 and 1991]. In the linearized problem the supercritical condition $U > c$ is interesting. In fact if $U < c$ then you could get the flat plate to fall straight down spontaneously, but in the supercritical case the plate must be restrained to keep it from turning broadside on. The solution of the supercritical problem is discussed in detail by Joseph [1990].

For the present purposes it will suffice to summarize the main results as cartoons shown in Figures 9 and 10. The main feature of interest for the tilt transition is the

● OSEEN LINEARIZATION OF THE GOVERNING EQUATIONS



$$\lambda U \frac{\partial \tau}{\partial x} + \tau = \eta[\nabla u + \nabla u^T]$$

$$\rho U \frac{\partial u}{\partial x} = -\nabla p + \text{div} \tau, \quad \text{div} u = 0$$

● VORTICITY IS GOVERNED BY A TELEGRAPH EQUATION, HYPERBOLIC WHEN $M > 1$

$$\frac{\partial^2 \omega}{\partial x^2} + \frac{\text{Re}}{M^2 - 1} \frac{\partial \omega}{\partial x} = \frac{1}{M^2 - 1} \frac{\partial^2 \omega}{\partial y^2}$$

● THERE IS A SHOCK OF VORTICITY.

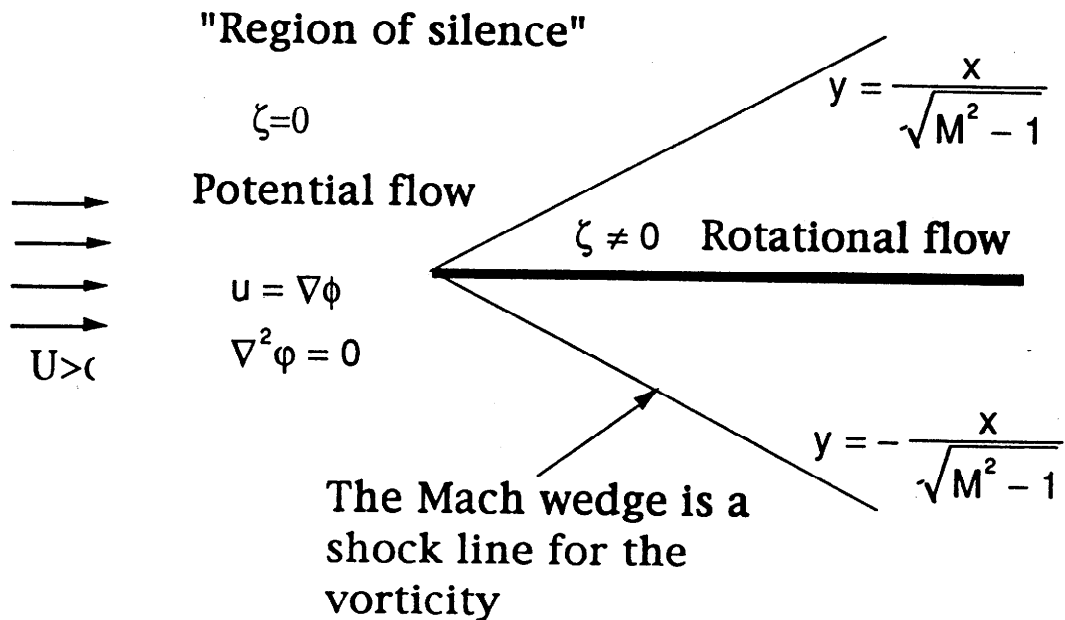
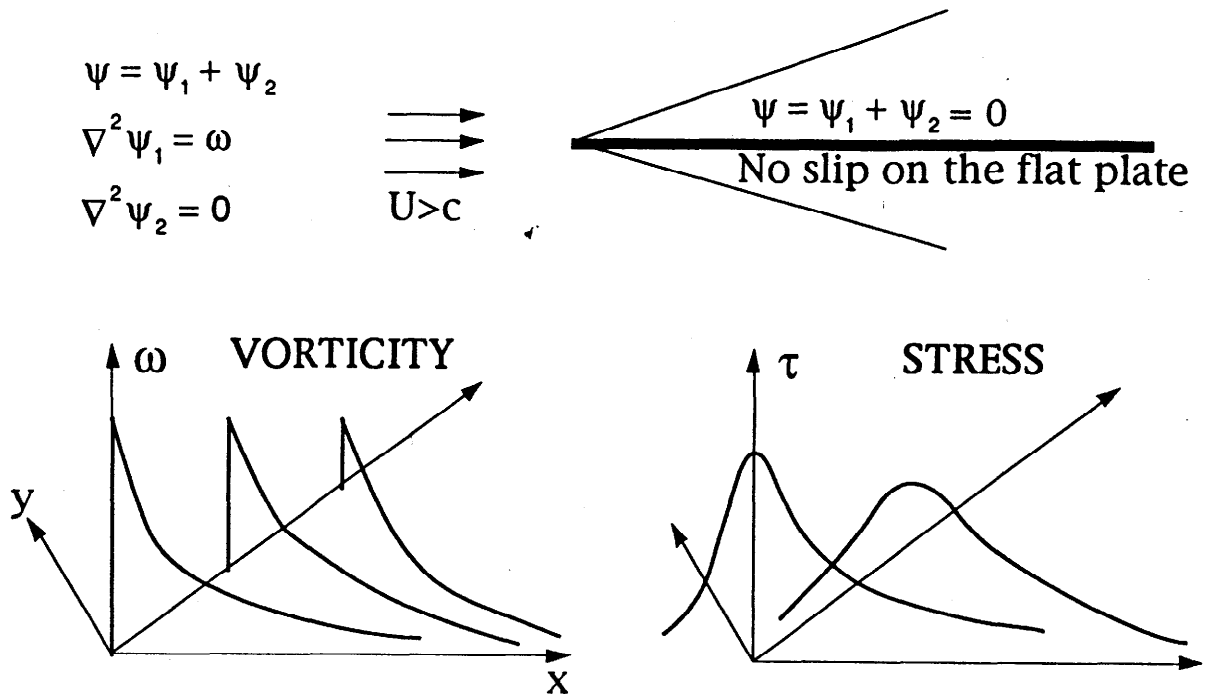


Figure 9. Linearized, partly hyperbolic flow over a flat plate.

- The vorticity ω is hyperbolic, but the stream function is elliptic.



- There is no upstream influence of vorticity.
- There is a big upstream influence on velocity.
- There is a big upstream influence on stress.
- You don't need nonlinear models for stress overshoot. Here, dynamics gives rise to the overshoot.
- The unconstrained plate is unstable and will undergo a tilt transition when $M > 1$.

Figure 10. Dirichlet problem for the flat plate.

How potential flow could enter into the tilt angle transition

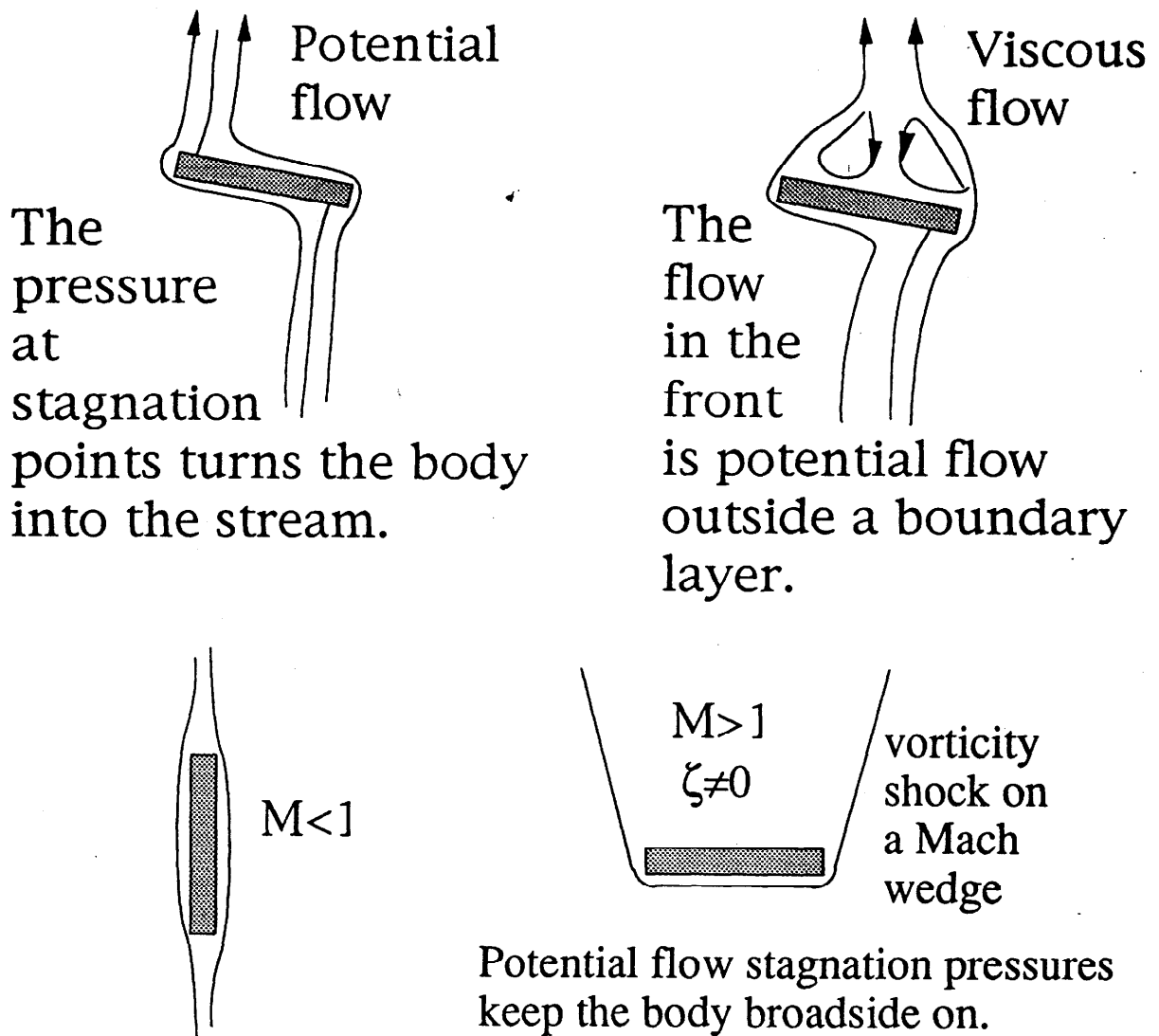


Figure 11. Conjecture concerning the way inertial pressures at the stagnation point at the front of a plate falling into a viscoelastic fluid at a speed $U > c$ will turn the plate broadside on.

emergence of potential flow on the front side of the plate. We saw already in Figures 3 and 4 that the potential flow on the front side of the body tends to destabilize configurations which are different than broadside on. The conjecture being advanced here is that the change prompts the kind of potential stagnation point flow on the front side of the plate that allows inertia pressures to turn the broadside of the flat plate into the stream, as in Figure 11.

5. Potential flow of a linear viscoelastic fluid

The cartoon's shown in Figures 9 and 10 already suggest that in the linearized case, potential flows are a solution of the equations of motion. We are talking about an Oseen linearization, perturbations from a uniform stream with speed U . In all such perturbations the stress is given by

$$\mathbf{S} = \int_{-\infty}^{\tau} G(t-\tau) \mathbf{A} [\mathbf{u}(\chi, \tau)] d\tau \quad (5.1)$$

where

$$\chi = \begin{bmatrix} x-U(t-\tau) \\ y \\ z \end{bmatrix} \quad (5.2)$$

and $G(s) = e^{-s/\ell}$ for Maxwell models. If

$$\mathbf{u} = \nabla \phi \quad (5.3)$$

is a potential flow now, and in the past, then

$$\mathbf{A} = \nabla \otimes \nabla \phi \quad (5.4)$$

and

$$\text{div } \mathbf{S} = \nabla \psi \quad (5.5)$$

where

$$\psi = \int_{-\infty}^{\tau} G(t-\tau) \nabla^2 \phi(\chi, \tau) d\tau = 0. \quad (5.6)$$

We get the same Bernoulli equation in inviscid, viscous or linearly viscoelastic potential flow

$$p = -\rho \frac{\partial \sigma}{\partial \tau} - \frac{\rho}{2} U^2 - \rho U \frac{\partial \sigma}{\partial x} - \rho \mathbf{g} \cdot \mathbf{x} - C(\tau) \quad (5.7)$$

where $C(\tau)$ is a spatially constant of integration. The stress then is given by

$$\mathbf{T} = -p \mathbf{1} + \mathbf{S}$$

where

$$\mathbf{S} = \int_{-\infty}^{\tau} 2G(t-\tau) \nabla \otimes \nabla \phi(\chi, \tau) d\tau. \quad (5.8)$$

6. Aknowledgements

This research was supported by the NSF, ARO and AHPCRC.

7. References

- Allen, E and Uhlherr, P.H.T. 1989 Nonhomogeneous sedimentation in viscoelastic fluids. *J. Rheology* **33**, 627-638.
- Ambari, A., Deslouis, C. and Tribollet, B. 1984 Coil-stretch transition of macromolecules in laminar flow around a small cylinder. *Chem. Eng. Commun.* **29**, 63-78.
- Brunn, P. 1977 The slow motion of a rigid particle in a second-order fluid. *J. Fluid Mech.* **82** (3), 529-550.
- Crochet, M.J. and Delvaux, V. 1990 Numerical simulation of inertial viscoelastic flow, with change of type, in *Nonlinear Evolution Equations that Change Type*. Springer-Verlag, New York.
- Fortes, A., Joseph, D.D. and Lundgren, T.S. 1987 Nonlinear mechanics of fluidization of beds of spherical particles. *J. Fluid Mech.* **177**, 467-483.
- Fraenkel, L.E. 1988 Some results for a linear, partly hyperbolic model of viscoelastic flow past a plate, in *Material Instabilities in Continuum Mechanics and Related Mathematical Problems* (ed. J.M. Ball). Clarendon Press, Oxford.
- Fraenkel, L.E. 1991 Examples of supercritical, linearized, viscoelastic flow past a plate. *J. Non-Newtonian Fluid Mech.* **38**, 137-157.
- Hermes, R.A. and Fredrickson, A.G. 1967 Flow of viscoelastic fluids past a flat plate. *AIChE J.* **13**, 253-259.
- Highgate, D.J. 1966 Particle migration in cone-plate viscometry of suspensions. *Nature*, **211**, 1390-1391; D.J. Highgate and R. W. Whorlow (Ed.), *Polymer Systems: Deformation and Flow*, Macmillan, London, 1968, 251-261.
- Highgate, D.J. and Whorlow, R. W. 1969 End effects and particle migration effects in concentric cylinder rheometry. *Rheol. Acta*, **8**, 142-151.
- Hu, H.H. and Joseph, D.D. 1990 Numerical simulation of viscoelastic flow past a cylinder. *J. Non-Newtonian Fluid Mech.* **34**, 347-377.
- Hu, H.H. and Joseph, D.D. and Crochet, M. 1992 Direct simulation of fluid particle motions. *Theor. Comp. Fluid Dynamics*. **3**, 285-306.
- Hu, H.H. and Joseph, D.D. and Fortes, A.F. 1992 Experiments and direct simulations of fluid particle motions. To appear in *Int. Video J. of Eng. Research* **3**.
- James, D.F. 1967 Laminar flow of dilute polymer solutions around circular cylinders, Ph.D. Thesis. Cal. Inst. Tech. Pasadena.
- James, D.F. and Acosta, A.J. 1970 The laminar flow of dilute polymer solutions around circular cylinders. *J. Fluid Mech.* **42**, 269-288.
- Joseph, D.D. 1985 Hyperbolic phenomena in the flow of viscoelastic fluids, in *Viscoelasticity and Rheology* (eds. A.S. Lodge, J. Nohel, and M. Renardy). Academic Press.

- Joseph, D.D. 1990 Fluid Dynamics of Viscoelastic Liquids, Applied Mathematical Sciences, 84, Springer-Verlag, New York.
- Joseph, D.D. 1992 Bernoulli equation and the competition of elastic and inertial pressures in the potential flow of a second order fluid. J. of Non-Newtonian Fluid Mech., 42, 385-389.
- Joseph, D.D., Arney, M.S., Gillberg, G., Hu, H., Hultman, D., Verdier, C. and Vinagre, T. M. 1992 A spinning drop tensioextensometer. J. Rheology 36, 621-662.
- Joseph, D.D., Liao, T.Y. and Hu, H.H. 1992 Drag and moment in viscous potential flow. European J. Mech. B/Fluids (to appear), see also AHPCRC preprint 92-058.
- Joseph, D.D., Matta, J. and Chen, K. 1987 Delayed die swell. J. Non-Newtonian Fluid Mech. 24, 31-65.
- Joseph, D.D., Narain, A. and Riccius, O. 1986 Shear-wave speeds and elastic moduli for different liquids. Part 1: Theory. J. Fluid Mech. 171, 289-308.
- Joseph, D.D., Nelson, J., Hu, H.H. and Liu, Y.J. 1992 Competition between inertial pressures and normal stresses in the flow induced anisotropy of solid particles. Proceedings of the XIth Int. Congress on Rheology, Brussels, Belgium, August 17-21.
- Joseph, D.D., Riccius, O. and Arney, M.S. 1986 Shear-wave speeds and elastic moduli for different liquids. Part 2: Experiments. J. Fluid Mech. 171, 309-338.
- Joseph, D.D., Singh, P., and Fortes, A. 1992 Nonlinear and finite size effects in fluidized suspensions in "particulate two-phase flow." (ed. M. Roco), Chapter 10, Butterworth.
- Leal, L.G. 1975 The slow motion of slender rod-like particles in a second-order fluid. J. Fluid Mech. 69, 305-337.
- Liu, Y.J. and Joseph, D.D. 1992 Sedimentation of particles in polymer solutions. AHPCRC preprint 92-076, University of Minnesota (to appear).
- Michele, J. Pätzold, and R. Donis, R. 1977 Alignment and aggregation effects in suspensions of sphere in non-Newtonian media. Rheol. Acta, 16, 317-321.
- Petit, L. and Noetinger, B. 1988 Shear-induced structure in macroscopic dispersions. Rheol. Acta, 27, 437-441.
- Thompson, W. and Tait, P.G. 1879 Natural Philosophy, 2nd Ed., Cambridge.
- Ultman, J.S. and Denn, M.M. 1970 Anomalous heat transfer and a wave phenomenon in dilute polymer solutions. Trans. Soc. Rheol. 14, 307-317.